SIMULATING THE CLIMATE SINCE 1000 AD WITH THE AOGCM ECHO-G

J. F.González-Rouco[1], E. Zorita[2], U. Cubasch[3], H. von Storch[2], I. Fisher-Bruns [4], F. Valero [1], J. P. Montávez[1], U. Schlese[4], and S. Legutke[4]

[1]Universidad Complutense Madrid, Spain,
[2]GKSS Research Center, Germany
[3]Freie Universitaet Berlin, German
[4]Max Planck Institute, Hamburg, Germany

ABSTRACT

Assessment of climate variability and changes through the last millennium is crucial for understanding and modeling current and future climate. Efforts have relied both in the statistical reconstruction of climate variability using proxy data and the numerical simulation of past climate states with the use of climate models.

Numerical simulations have used models and experiments of varying complexity and design mostly focused on the impacts of solar variability on climate. This work explores the response of a *state-of-the-art* global atmosphere-ocean climate model to changes in external forcing. The analysis focuses on two long climate integrations with the ECHO-G global climate model (MPI, Hamburg) in which the external forcing has been gradually changed along the simulations according to the estimations of changes in the solar irradiance, atmospheric reflectivity due to volcanic eruptions and the concentrations of greenhouse gases. One of this integrations (FOR1) covers the period AD 1000 to 1990 and a second integration (FOR2) spans the period 1550 to 1990 A. D.

Key words: General Circulation Models; transient integrations; solar forcing; anthropogenic forcing.

1. INTRODUCTION

The assessment of the recently observed climate warming and its potential relation to an anthropogenic action has prompted the need to understand and estimate climate changes through the last millenium (Jones et al., 2001). Efforts have relied both in the statistical reconstruction of climate variability using proxy data and the numerical simulation of past climate states with the use of climate models.

Reconstructions of the climate history through the last millenium have used a variety of proxy indicators (Jones et al., 1998). These studies have focused in a wide range of spatial scales: from the local and regional (Cook, 1995) to hemispherical and global scales (Briffa et al., 1998; Mann et al., 1999). Though most efforts have been devoted to the reconstruction of past temperature variability (Jones et al., 1998; Mann et al., 1999; Huang et al., 2000; Esper et al., 2002; Briffa and Osborn.,2002), a great deal of reseach has also concentrated in reconstructing hydrological and atmospheric circulation indices (Villaba et al., 1998; Luterbacher et al., 2002). Such effort has suggested the existence of interesting broad climate anomalous periods like the warmer Medieval Optimum (MO) and the colder little ice age (LIA) (Jones et al., 2001). Inside the LIA the Late Maunder Minimum (LMM) and the Dalton Minimum (DM), arise as periods of reduced solar activity which could have had a direct implication in climate (Crowley, 2000; Lean, 2000). Still, much discussion is going on concerning the reliability and implications of the available reconstructions (Mann and Hughes, 2002; Cook and Esper, 2002; Mann et al., 2003)

Numerical simulation has used models and experiments of varying complexity and design mostly focused on the impacts of solar variability on climate (Haig, 1999 and references therein). Crowley (2000), showed results with an energy balance model supporting the idea that the last centuries of global warming cannot be fundamented solely on changes in natural variability and solar forcing. Shindell's et al. (2001) time slice integrations for the LMM with a global climate model (GCM) including a 'state-of-the-art' atmospheric component and a mixed layer ocean suggest that changes in regional temperature for the LMM can be driven by anomalous circulation regimes induced by changes in solar variability. The population of transient integrations with 'state-of-the-art' GCMs is smaller due to computational limitations. Cubasch et al. (1997) presented integrations with a coupled atmosphere-ocean GCM forced with the estimations of solar forcing since 1700 A. D. The surface temperature response pattern was dominated by the land-sea contrast and broadly resembled the pattern obtained in greenhouse-gas sim-

ulations (Hegerl et al., 1997). The warming in the lasts centuries was smaller than in the observations. Rind et al. (1999) showed an ensemble of experiments with a lower resolution GCM coupled to a simplified ocean indicating also that the solar forcing is not sufficient to produce the rapid warming of the last decades.

With the perspective of the existent population of GCM runs, there is still a lack for numerical integrations which involve the effect of external forcings of different nature (natural and anthropogenic). This paper explores the surface temperature response of a *state-of-the-art* atmosphere-ocean GCM to changes in the external forcing (solar irradiance, volcanoes and greenhouse gases). Section 1 describes the temporal behaviour of the model in a simulation with constant external forcing and in two simulations driven with the estimations of past external forcings (solar irradiance, volcanic activity and greenhouse gasses). Section 2 is devoted to picture the relationship between solar and volcanic forcing and the temperature response in the forced simulations. Finally, some conclusions are summed up in Section 3.

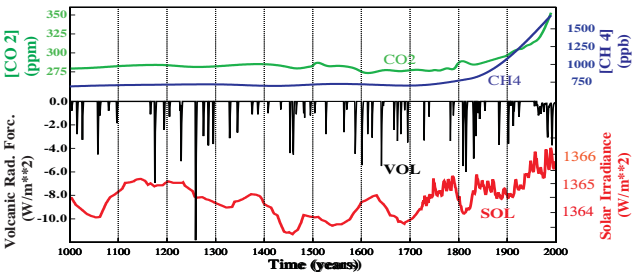

Figure 1. Estimations of greenhause gasses (CO2,CH4), solar irradiance (SOL) and changes in atmospheric reflectivity in the stratosphere (VOL) used to force the model.

2. MODEL AND EXPERIMENT DESIGN

The integrations have been produced with the ECHO-G atmosphere-ocean GCM (Legutke and Voss, 1999). This model consists of the spectral atmospheric model ECHAM4 (Roeckner et al., 1996) and the ocean model HOPE-G (Wolf et al., 1997), both developed at the Max Planck Institute of Meteorology in Hamburg . The atmospheric component constitutes a newer version of that used in Cubash et al. (1997) and is used with a horizontal resolution T30 (aprox. $3.75^o \times 3.75^o$) and 19 vertical levels. The horizontal resolution of the ocean model component is about $2.8^o \times 2.8^o$ with a grid refinement in the tropical regions. Vertical discretization incorporates 20 levels. A constant in time flux adjustment was applied o avoid climate drift.

Results are shown for three simulations with ECHO-G. In a control (CONT) simulation the external forcing was kept constant in time and set to the values of the present climate. The model was integrated for 1000 years. The other two integrations were made driving the coupled model with estimations of three past external forcing factors: solar variability, greenhouse gas concentrations in the atmosphere and an estimation of the radiative effects of stratospheric volcanic aerosols. No changes in the anthropogenic atmospheric aerosol concentrations have been considered. The two forced integrations cover the period 1000 to 1990 A.D. and 1550 to 1990 A. D. (FOR1 and FOR2, respectively).

Figure 1 shows the estimations of the forcing factors used to drive the model. The atmospheric concentrations of carbon dioxide and methane were estimated from analysis of air bubles in Antartica ice cores (Blunier et al., 1995; Etheridge et al., 1996). The past variations of solar output were derived from observation of sun spots and concentrations of the cosmogenic isotope ^{10}Be (Lean et al., 1995). The effect of volcanic aerosols is included as global annual estimations of atmospheric optical depth translated to short wave radiative forcing (Sato et al., 1993). Thus, the experiments presented herein make use of the same datased used by Crowley (2000) to force his energy balance model. The trends in the greenhouse gasses after 1800 A.D. are apparent as well as that in solar forcing. The higher solar irradiance in the MO and lower values in the LIA, as well as shorter anomalous periods within the LIA like the Spoorer Minimum (aprox. 1450 A.D.), the LMM (aprox. 1700 A.D.) and the Dalton Minimum (aprox. 1800 A. D.) are also evident.

FOR1 (FOR2) was started from initial conditions extracted from the control simulation and driven in a period of 100 years (35 years) to the forcing conditions of 1000 A. D. (1500 A. D.). In order to avoid potential contamination of the first decades of the integration in FOR2 from the relatively short *spin down* period, results will be shown here focussing on the time interval 1550 to 1990 A. D. Further description and results with these simulations are specified in Zorita and González-Rouco, (2002) and Zorita et al. (2003a; 2003b).

3. TEMPERATURE RESPONSE

Figure 2 shows the global temperature anomalies for the control and forced simulations (reference period was 1960-1990; dates are arbitrare for the 1000 yr control simulation). The control simulation is fairly stable in time. Maximum trends of the order of 0.025 K/dec occur in the second and third century of the simulation and also in the last two centuries. The forced simulations show a more complex structure in response to the imposed external forcing. FOR1 simulates a climate comperable to CONT (present-day climate) during the first centuries of the simulation and after that a colder climate up to the 19th century. FOR2 is in remarkably good agreement for the overlapping period (correlation 0.82; $p < 0.05$). The

warmer climate at the beginning of FOR1 is consistent with the existence of a MO. After the 11th century a persistent cooling trend of about 0.01 K/dec is evident which gives way for the last two centuries (both in FOR1 and FOR2) to a warming rate of about 0.04 K/dec. The cooling episode is consistent also with the existence of a LIA cooling in the proxy reconstructions (Mann et al., 1998). Inside the simulated LIA, three anomalous periods arise which match in timing with the Spoorer Minimum (SM), the LMM and the DM (SOL, Fig. 2). During these episodes, abrupt coolings appear of the order of 0.2 K/dec.The overall degree of variability is also higher in the forced integrations than in the control integration (the ratio of variances forced vs. control is 5.9 for FOR1 and 6.8 for FOR2).

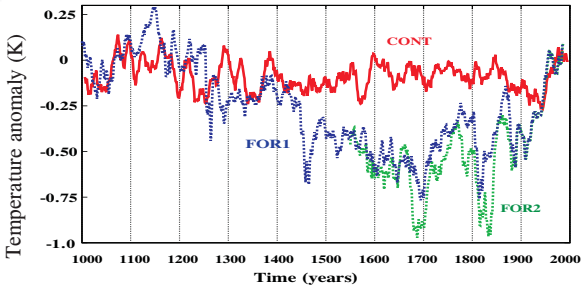

Figure 2. Global temperature anomalies for the control (CONT) and two forced simulations with the ECHO-G model (FOR1 and FOR2). Reference period is 1960 to 1990 A. D. Dates are arbitrare and do not correspond to actual dates in the CONT simulation.

Figure 3 shows hovmoller diagrams with the temporal evolution of the latitudinal anomalies throughout the period of integration (reference periods as in Fig. 2). CONT shows again a fairly stable behaviour in time. The Northern Hemisphere (NH) tends to be usually warmer than the Southern Hemisphere (SH), a reasonable feature keeping in mind the higher fraction of land areas in the NH. FOR1 and FOR2 depict the latitudinal extension of the temperature anomalies shown in Fig. 2. Both simulations show regional warming in the high latitudes of the Southern Hemisphere, probably due to ocean-atmosphere interactions. This warming enhances the global warm temperature anomalies in FOR1 during the MO-like period and progressively cools down through the 1000 years of simulation. The NH responds with a regional warming comparable to the climate state in the 20th century. The coldest conditions during the LIA-like simulated period are attained mostly in the high latitudes of the NH and spread almost globally and. Changes of 1K are apparent in the NH averages (not shown) in remarkably short periods (3 decades) during the simulated SM, LMM and DM.

In the last two centuries FOR1 and FOR2 experience warming trends as a response to the increase in greenhouse gasses and solar irradiance (CO2, CH4 and SOL). Cubasch et al. [1997] pointed that the previous version of this model reacted with a trend

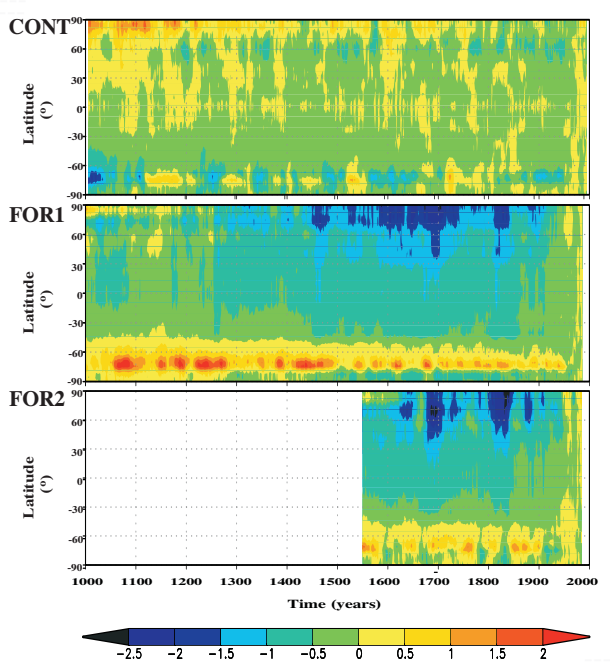

Figure 3. Hovmoller diagrams for the latitudinal temperature anomalies in the control and forced integrations (reference periods as in Fig. 2).

of about 0.02 K/dec. Global averages present in this simulation a warming rate of 0.038 K/dec since 1850. Thus, speculative values can be provided for this simulation of about 50% of the warming related to the increase in greenhouse gasses. However, for a more thorough study in this sense an ensemble of simulations is needed taking into account the isolated impact of each forcing factor.

A comment is also worth on the similitude of the simulated global and hemispheric changes to the proxy reconstructions. Correlation of global averages in FOR1 (FOR2) with 5-yr low pass filtered global temperature reconstructions of Jones et al. (1998) for the 1550-1990 interval is 0.75 (0.76) ($p < 0.05$). The correlation of FOR1 with reconstructed temperature for the 1000-1990 interval is 0.63. For the NH the relationship is also good, for instance correlations of FOR2 (NH averages) with the NH reconstructions of Mann et al (1998) is 0.6 ($p < 0.05$) for the 1550-1990 interval. The degree of warming is however larger in the model simulation than in the reconstructions. The question still remains of whether this is a result of infraestimation of variability on the side of the reconstructions (Mann and Hughes, 2002; Cook and Esper, 2002; Mann et al., 2003) or a problem of climate sensibility in the model. This last issue calls for an ensemble of model simulations for different initial conditions with different models. Preliminary results indicated a similar behaviour in a simulation forced with solar irradiance using the Hadley Center Model (Widmann and Tett, 2003).

Figures 4 and 5 allow for a combined espatial and temperal description of the changes through the simulations. For each simulation, results for the first

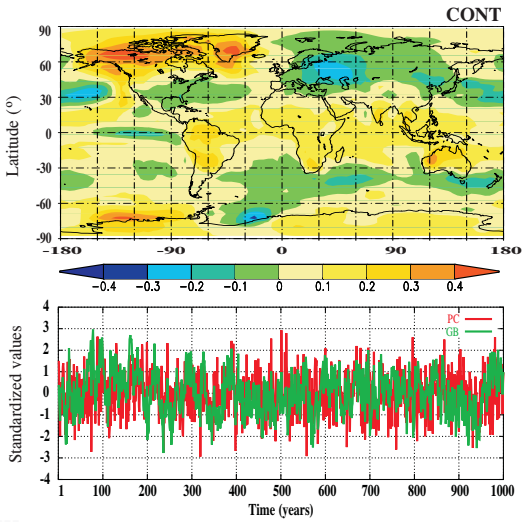

Figure 4. Results from the EOF analysis of annual surface temperature in the 1000 year control run: (MAP) First empirical orthogonal function; (series) first principal component (PC) and global averages (GB). This EOF accounts for 9.3 % of the total variance.

mode of an empirical orthogonal function (EOF) analysis (Preisendorfer, 1988) are shown. The patterns were derived from standardized temperature time series and were subsequently rescaled by the local standard deviation. The control simulation presents an EOF pattern (Fig. 4) comparable to that of Zorita et al. (2003a). The northern latitudes of both hemispheres show the highest amount of variability. Also, the tropical regions show high values, possibly related to the higher horizontal surface irradiance in this areas. The corresponding principal component (PC) is shown in Fig. 4 and also, for comparison, the time series of global averages.The correlation between them is 0.53 ($p < 0.05$). Both time series show variability in annual to century long timescales.

Figure 5 illustrates the changes in this first EOF mode when the external forcing is imposed. The variances accounted for by the first EOF in FOR1 and FOR2 are 30% and 28.8%, respectively. Both, FOR1 and FOR2 respond with a pattern of variability which on the global scale describes land-sea contrasts, with the warming occurring mostly over the continents. This structure is reminiscent of that in the pattern of variance for surface temperature in the three simulations (not shown) which presents higher ammounts of variability over the continents and higher latitudes in each hemisphere. Therefore, this suggests that the first reaction of the system to the changes in the external forcing is to excite the land-sea contrasts. The higher latitudes of the NH show the strongest warming, distributed mainly over northern Europe and the area from the Hudson Bay to western Greenland. The higher latitudes of the SH hemisphere respond with some cooling anomalies in agreement with Fig. 2. The variances accounted for by the first EOF in FOR1 and FOR2 are 30% and 28.8%, respectively.

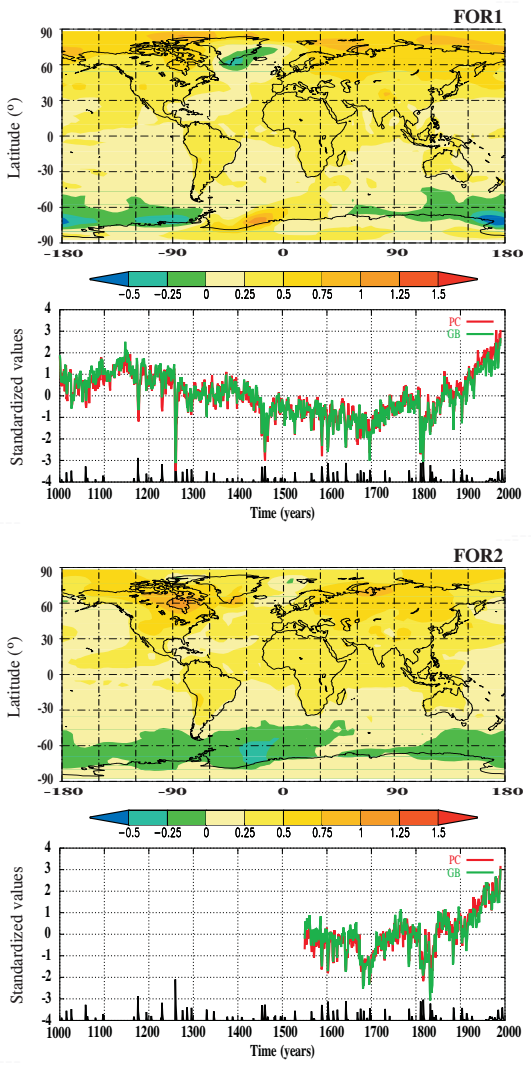

Figure 5. Results from the EOF analysis of annual surface temperature in the forced integrations: (MAPs) First empirical orthogonal function; (series) first principal component (PC) and global averages (GB). The black line shows for comparison the moments of the volcano eruptions as in Fig. 1. This EOF accounts for 30.0 % and 28.8 % of the total variance in FOR1 and FOR2, respectively.

The time series in Fig. 5 show a close relationship between the first principal component (PC) in each analysis and the associated time series of global averages (GB). Correlations are 0.97 (FOR1) and 0.95 (FOR2). Thus, changes in temperature in both simulations are well described by the first EOF mode. It can be noted that the response to external forcing introduces a higher amount of variability on centennial timescales, as will be discussed later. Changes in the volcano eruptions are also shown along with the time series in Fig. 5 pointing a good agreement with secondary minima in the temperature evolution. FOR1 and FOR2 respond with a similar behaviour through the period 1550 to 1990 (correla-

tion 9.0). This feature, together with the spatial similarity of both EOFs in FOR1 and FOR2 suggests there is a robust spatial pattern of response to forcing which describes well century long changes which encompass the simulation of realistic relevant climate anomalous periods as the Medieval Optimum and the Little Ice Age, including the SP, LMM and DM. Also, this mode is capable of accounting for the warming trends in the last two centuries of the simulations, which should be partially related to the anthropogenic forcing. Thus, these results suggest there is a unique spatial pattern of temperature response which is able to resume the main aspects of the simulated climate variations for the period 1000 to 1990 A. D., including both the effects of non anthropogenic (before 1800 A. D.) and antropogenic (after 1800 A. D.) external forcing. Further robustness to this reasoning comes from comparison with other works, since the spatial patterns shown in Figures 4 and 5 are coincident with those obtained in the solar forced simulations for the last 3 centuries of the millenium of Cubasch et al. (1997) and also in those of future greenhouse scenarios (Hegerl et al., 1997).

A comment is also worth on the differences between the first EOF simulated by FOR1 and FOR2. Such differences can be appreciated mainly on a regional basis in the higher latitudes of each hemisphere. This feature suggests there can be other mechanisms related to natural variability in the atmospheric dynamics of each simulation (i.e. the Artic and Antarctic Oscillations, North Atlantic Oscillation, etc) which can play a role in producing a somewhat different regional response in each simulation. A further comment can be made on the spatial fingerprint of the anthropogenic forcing in the last centuries of the simulation. Detection of this effect would require an appropriate optimal detection technique (Hegerl et al., 1997), which, so far, is beyond the scope of this text.

4. RELATIONSHIP WITH SOLAR FORCING

This section explores the relationship between the solar irradiance used to force the model and the simulated temperature response in FOR1 and FOR2. Results in Figs. 2,3,5 show there is a good correspondence of the temperature response of the model to solar forcing. The correlation between changes in irradiance (SOL, Fig. 1) and global temperature in FOR1 and FOR2 is 0.60 and 0.62 ($p < 0.05$), respectively. Both global temperature averages in Fig. 2 show good agreement (correlation 0.82) for the overlaping period (1550 to 1990 A. D.). Therefore, about 40 % of variance is shared between solar irradiance and temperature. A value comparable to that obtained by Cubasch et al. (1997). Figure 6 ilustrates this relation with the correlation field between SOL (Fig. 1) and grid point simulated temperature in FOR1 for the period 1000 to 1990 A. D. The pattern shows maximum values over the ecuatorial and tropical regions corresponding to areas of higher horizontal surface irradiance (see also Fig. 4). The correlation map of global temperature averages in all simulations and grid point temperature (not shown) bears a similar structure.

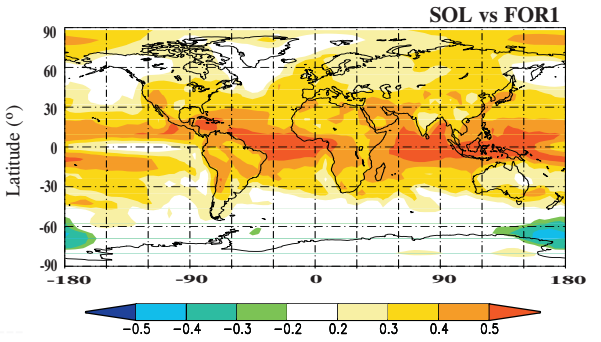

Figure 6. Field correlations between SOL (Fig. 1) and annual gridpoint tempertature in FOR1.

Comparison of Fig. 1 and Fig. 2 suggests that there could be some lagged response between solar irradiance and the temperature response. This is illustrated in Figure 7 where correlations are shown between zonal meen values of FOR1 simulated temperature and solar irradiance (SOL) as a function of time lag. The results are comparable to Cubasch et al. (1997) and show high correlations mostly over the tropics and for timescales up to 20 years. Correlations decrease and even turn to negative at higher latitudes. This delayed behaviour is consistent with the slower response of the oceans and the significant autocovariance in time scales of 10 to 20 years associated to the solar activity cycle. Fig. 7 shows lagged correlation maps for global gridpoint temperatures, ocean and land areas. In agreement with the previous statement, the response of the ocean masses embodies longer timescales than the response of the land areas.

Figure 8 shows the actual effective solar constant used to drive the model in FOR1 and FOR2. As stated in section 2, the volcanic forcing was introduced as the equivalent short wave modification in the solar constant as in Crowley (2000). The statistical spectral properties of the effective solar constant and the *raw* solar irradiance are shown in Figure 9 (top panel) together with the spectrum of global temperature averages in FOR1.

Comparison of solar irradiance (SOL) and effective solar irradiance (Eff. SOL) spectrum estimates in Figure 9 yield a higher proportion of variance accumulated in high frecuencies for Eff. SOL, a reasonable resault since the effective solar forcing introduced in the model includes the shorter timescale influence of the volcanic eruptions. In SOL, an accumulation of variance in timescales centered in 11 years is also apparent. This is consistent with the presence of the solar activity cycle in the reconstructions of solar irradiance after the 18th century (see SOL in Fig. 1). This signal stands out of a first order

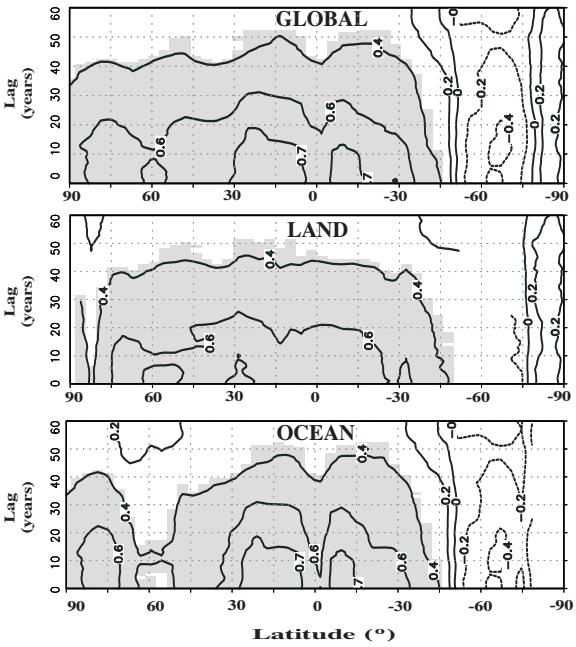

Figure 7. Latitudinal temperature averages vs. solar irradiance time-lag correlation coefficients in the FOR1 simulation for global gridpoint temperatures, land-masked temperatures and ocean-masked temperatures. Shading indicates significance ($p < 0.05$), accounting for autocorrelation.

autoregressive process spectrum (not shown) and is masked in the spectrum of Eff. SOL due to the presence of volcanic forcing which produces a rather flat spectrum in medium to high frequencies. In the same panel of Fig. 9 the normalized spectrum of FOR1 compares quite well with the Eff. SOL spectrum for medium to low frequencies. The closer relationship to Eff. SOL than to *raw* SOL is reasonable based on the fact that the forced simulations are actually driven with Eff. SOL. The closer relationship with Eff. SOL at low and medium frequencies is also sensible since at higher frequencies other mechanisms related to internal variability in the system can play a more relevant role.

The lower panel in Fig. 9 shows a comparison of the temperature spectra in the three simulations. Two evident features arise in this analysis: firstly, both forced simulations produce a similar spectrum in low to medium frequencies, up to periods of about 4 years, as a response to the common external forcing and in agreement with the high correlations (0.82) between FOR1 and FOR2; secondly, both forced simulations show a higher proportion of variance in low frequencies than in high frequencies in comparison to CONT. Thus, the imposed external forcing basically boosts the amount of variance in this timescales of the spectrum, a feature which was straight forward derived from Fig. 2.

A final illustration of the relation between simulated global temperatures in FOR1 and FOR2 with the effective solar forcing is presented in Figure 10 where cross spectra of Eff. SOL and global temperature averages are shown. High coherence values are obtained for long timescales down to periods of about 4 years (frequency: 0.25 yr^{-1}) in correspondence with the results in the lower panel of Fig. 9. The phase keeps fairly stable in both cases, though with a clear displacement showing the lag of temperature respect to solar forcing, as stated in the comments to Fig. 7.

Sumarizing, the long term temperature response in the forced simulations is in good agreement with the forcing imposed to the model and supports that the simulated MO and LIA are radiatively induced. Since both FOR1 and FOR2 show a comparable response, these results show robustness regardless of the initial conditions in each simulation.

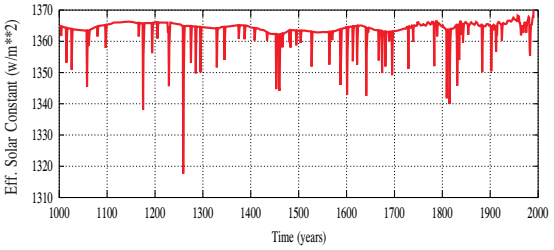

Figure 8. Effective solar irradiance from Crowley et al. (2000) used to drive ECHO-G. Volcanic forcing was introduced as equivalent reduction of short wave radiation by each volcanic eruption.

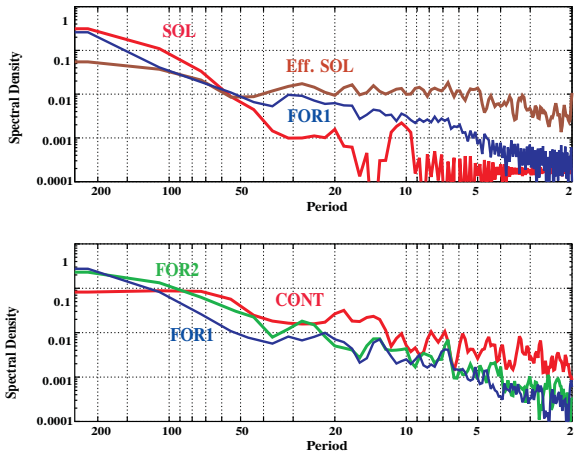

Figure 9. Normalized spectra of solar constant (SOL), effective solar constant (Eff. SOL) and global temperature averages in CONT, FOR1 and FOR2. All spectra are calculated for the 1000 to 1990 A. D. perido except for the FOR2 values (1550 to 1990 A. D.)

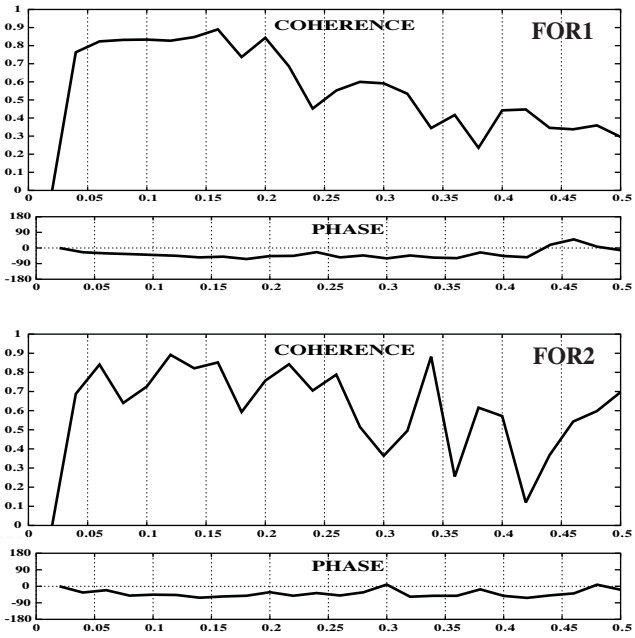

Figure 10. Cross spectra of effective solar constant and global temperature averages in FOR1 and FOR2

4.1. Solar activity cycle

The previous description aimed at picturing the general behaviour of the solar forcing and the temperature response in the spectral space. One issue which has received considerable attention is the variability in solar irradiance related to the 11 year solar acitivity cycle and its potential relationship to Earth temperature (Friis-Christensen and Lassen, 1991; Lean, 2000). The following results are devoted to a concise description of the behaviour of the variability in forcing and simulated temperature series within the frequency band of the spectrum corresponding to the 11 yr solar activity cycle. In Figure 9 some power in solar irradiance (SOL) in time scales of 11 years is noticeable. This power stands out of the 0.05% level of significance in a comparison with the spectral power associated to an AR1 process with the same degree of autocovariance as in SOL. This does not happen for the effective solar constant (Eff. SOL in Fig. 9) which produces a rather flat spectrum in this frequency bands as an effect of the contamination of variance from the volcanic episodes. In the temperature spectra in Fig. 9 there is also no evident accumulation of variance around the 11 year signal.

In spite of the relatively low variance accumulated, it is interesting to understand how the model responds in these timescales to the imposed solar forcing. Figure 11 shows the spectra for SOL and Eff. SOL as in Fig. 9 and the transfer function of a band pass filter used to isolate the signal centered in timescales around 11 years. The filter uses least squares coefficients to reduce Gibbs oscillations (Bloomfield, 1976; von Storch and Zwiers, 1999) with cutoff periods in 8 and 16 years and 70 terms, which implies a loss of 70 values at the begginning and end of the original series. The transfer function of the filter is indicated in Figure 11. The contribution of the Gibs oscillations is avoided in the picture for clarity.

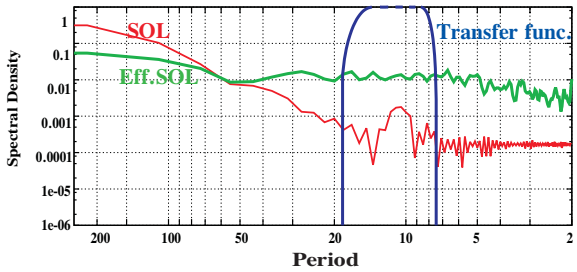

Figure 11. Spectra of solar constant (SOL) and effective solar constant (Eff. SOL) as in Fig. 9. Transfer function of the band pass least squares filter centered around 11 years.

The band-pass filtered outputs (SOL FILT, Eff. SOL FILT) of the solar and effective solar irradiance are shown in Fig. 12 (top panel). In the case of SOL, the variability in the selected frequency interval arises in the 18th century when the time series of the reconstructed solar irradiance (Crowley, 2000) incorporates the changes associated to the 11 year sunspot cycle. In the case of Eff. SOL, there is contribution to variance in timescales of 11 years throughout the whole period from 1000 to 1990 A. D. This variability can only come from the contribution of the volcanic eruptions. This is illustrated in Fig. 12 (middle and botton panel) where the filter outputs of solar and effective solar irradiance (SOL FILT, Eff. SOL FILT) are compared with standardized versions of the original forcing series (SOL, Eff. SOL)for the period 1500 to 1990 A.D. It is apparent that in the case of SOL (middle panel), there is good agreement between the timing of the oscillations in the filter outputs and the occurrence of 11 year solar activity cycles. In the case of the effective solar forcing it is evident that the changes in the filter outputs are well in phase with the ocurrence of volcanic eruptions. The amplitude of the oscillations seems to be also related with the intensity of volcanic eruptions. This supports the idea that the rather medium to high frequency flat spectrum of Eff SOL in Figure 11 comes from the contribution of volcanic eruptions to these timescales. Since the forced simulations incorporate the volcanic forcing, it can be expected that FOR1 and FOR2 respond in these timescales to the forcing indicated in Eff. SOL FILT rather than SOL FILT.

The filtered global averages for the control and forced integrations are shown in Figure 13. This figure suggests that the control simulation produces variability in timescales centered in 11 years regardless of the solar forcing being constant for this simulation. Thus, internal natural variability in the climate system is able to produce variance (noise) in this timescales. An interesting feature that concerns the forced simulations is that these respond well in agreement with

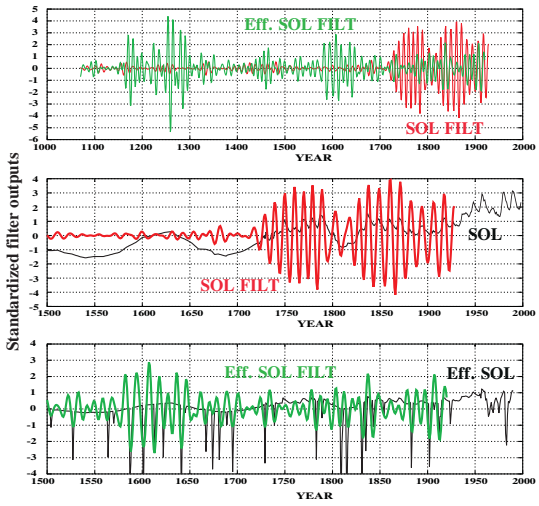

Figure 12. 11 year centered band-pass filter outputs of SOL and Eff. SOL. (Top panel) Comparison of filter outputs of SOL and Eff. SOL. (Midel panel) Comparison of original input and output of the band-pass filter for SOL. (Botton panel) As in midle panel for Eff. SOL.

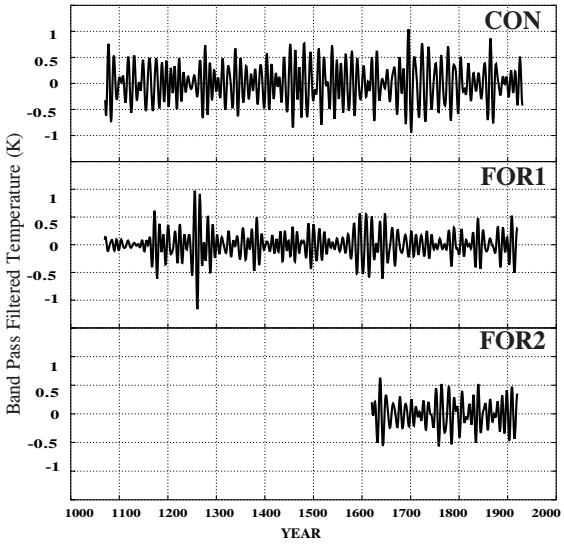

Figure 13. 11 year centered band-pass filter outputs for global temperature averages in the control and forced integrations.

the filter outputs of Eff. SOL. It can be noticed that the filter output of FOR1 (Fig. 13 middle)agrees for the period 1000 to 1990 A.D. with the evolution in Eff. SOL FILT (Fig. 12 top). The correlation of the filtered temperature series in FOR1 (FOR2) with the filter output of Eff. SOL is 0.57 (0.42). Both correlations are significant accounting for the loss in degrees of freedom. The correlation map between the temperature filter outputs (Fig. 13) and gridpoint temperature anomalies in each integration leads to structures similar to that in Fig. 6 (not shown). Thus, these results suggest that for the forced integrations, the variability in timescales of 11 years imposed by the effective solar forcing modulates the temperature response.

5. CONCLUSIONS

The analysis of two climate simulations covering the last 1000 years with the model ECHO-G driven with the estimations of past external forcings (solar irradiance, volcanic activity and greenhouse gasses) reveals a temperature response which is largely in agreement with changes in solar irradiance. A MO-like and a LIA-like period are simulated as well as cooling anomalous periods coincident with the LMM and DM. Warming trends through the 19th and 20th centuries are larger than in previous simulations forced only with solar irradiance and seem to overestimate also most proxy-based climate reconstructions.

The spatial and temporal characteristics of the temperature response are well described by the first EOF mode of global surface temperature. This mode accounts well for the natural variability before industrialization and the partially induced anthropogenic warming in the last two centuries. The first eigenvector broadly resembles patterns of temperature change obtained both in paleoclimate simulations forced with solar irradiance and those of future greenhouse scenarios, showing a global land-sea contrast behaviour and most warming associated to the northern latitudes of the NH.

Analysis of the variability associated to time scales of 11 years reveals that the control, unforced, climate is able by itself to produce variability in this timescales, associated to the internal dynamics of the system. It is found that the imposed solar and volcanic forcing play the role of modulating changes in these timescales in the forced simulations.

ACKNOWLEDGMENTS

This work was partially funded by the DEKLIM Program of the German BMBF and by the project REN-2000-0786Cli of the spanish CICYT.

REFERENCES

Blunier, T., J.A. Chappellaz, J. Schwander, B. Stauffer, and D. Raynaud, Variations in atmospheric methane concentration during the Holocene epoch. *Nature* 374, 46–49, 1995.

Briffa, K. R., and T. J. Osborn, Blowing Hot and Cold, *Science, 295*, 2227–2228, 2002.

Bloomfield, P., Fourier Analysis of Time Series: an Introduction *John Wiley & Sons*, New York, 1976.

Briffa, K. R., F. H. Schweingruber, P. D. Jones, T. J. Osborn, S. G. Shiyatov, and E. A. Vaganov, Reduced Sensitivity of Recent Tree-Growth to Temperature at High Northern Latitudes, *Nature,* 391, 678–682, 1998.

Cook, E. R., Temperature Histories from Tree Rings and Corals, *Clim. Dyn.*, 11, 211–222,1995.

Cook, E. R., and J. Esper, Response to Tree-Ring Chronologies and Climate Variability, *Science*, 296, 848–849, 2002.

Crowley, T. J., Causes of Climate Change Over the Past 1000 Years, *Science*, 289, 270–277, 2000.

Cubasch, U., R. Voss, G. C. Hegerl, J. Waszkewitz, and T. J. Crowley, Simulation of the Influence of Solar Radiation Variations on the Global Climate with an ocean-atmosphere general circulation model, *Clim. Dyn.*, 13, 757–767, 1997.

Esper, J., E. R. Cook, and F. Schweingruber, Low-Frequency Signals in Long Tree-Ring Chronologies for Reconstructing Past Temperature Variability, *Science*, 295, 2250–2253, 2002.

Etheridge D., L.P Steele, R.L. Langenfelds, R.J. Francey J.M. Barnola, and V.I. Morgan, Natural and anthropogenic changes in atmospheric CO2 over the last 1000 years from air in Antarctic ice and firn. *J. Geophys. Res.*, 101, 4115–4128, 1996.

Friis-Christensen, E. and K. Lassen, Length of the Solar Cycle: An Indicator of Solar Activity Closely Associated with Climate, *Science*, 254, 698–700, 1991.

Haig, J. D., Modelling the impact of solar variability on climate, *J. Atmos. and Solar-Terrestrial Phys.*, 61, 63–72, 1999.

Hegerl, G. C., Multi-fingerprint Detection and Attribtion Analysis of Greenhouse Gas, Greenhouse gas-plus-aerosol and solar forced climate change, *Dlim. Dyn.*, 13, 613–634, 1997.

Huang, S., H. N. Pollack and P. Y. Shen, Temperature Trends over the Past Five Centuries Reconstructed from Borehole Temperatures, *Nature*, 403, 756–758, 2000.

Hurrell, J. W., Decadal Trends in the North Atlantic Oscillation: Regional Temperatures and Precipitation, *Science*, 269, 676–679, 1995.

Jones, P. D., K. R. Briffa, T. P. Barnett, and S. F. B. Tett, High-resolution paleoclimatic records for the last millenium: interpretation, integration and comparison with General Circulation Model control-run temperatures, *The Holocene*, 8, 455–471,1998.

Jones, P. D., T. J. Osborn, and K. R. Briffa, The Evolution of Climate Over the Last Millennium, *Science*, 292, 662-667, 2001.

Lean, J., J. Beer, R. Bradley, Reconstructions of solar irradiance since 1610- implications for climate change, *Geophys. Res. Lett.*, 22, 3195–3198, 1995.

Lean, J., Evolution of the Sun's Spectral Irradiance Since the Maunder Minimum, *Geophys. Res. Lett.*, 27, 2425–2428, 2000.

Legutke, S., and R. Voss, The Hamburg Atmosphere-Ocean Coupled Circulation Model ECHO-G Technical report, No 18, German Climate Computer Center (DKRZ), Hamburg.1999.

Luterbacher, J., E. Xoplaki, D. Dietrich, P.D. Jones, T.D. Davies, D. Portis, J.F. Gonzalez-Rouco, H. von Storch,D. Gyalistras, C. Casty, and H.Wanner, Extending North Atlantic Oscillation Reconstructions Back to 1500, *Atmos. Sci. Lett*, 2, 114–124, 2002.

Mann, M. E., R. S. Bradley, and M. K. Hughes, Global-Scale Temperature Patterns and Climate Forcing over the Past Six Centuries,*Nature*, 392, 779–787, 1998.

Mann, M. E., R. S. Bradley, and M. K. Hughes, Northern Hemisphere Temperatures During the Past Millenium: Inferences, Uncertainties and Limitations, *Geophys. Res. Let.*, 26, 759–762, 1999.

Mann, M. E., and M. K. Hughes, Tree-Ring Chronologies and Climate Variability, *Science*, 296, 848, 2002.

Mann, M. E., S. Rutherford, R. S. Bradley, M. K. Hughes, and F. T. Keiming, Optimal Surface Temperature Reconstructions Using Terrestrial Borehole Data, *J. Geophys. Res.,* 108, DOI 10.1029/2002JD002532, 2003.

Preisendorfer, R. W., Principal component analysis in meteorology and oceanography, Elsevier, C. D. Mobley, Amsterdam, 1988.

Rind, D., J. Lean, and R. Healy, Simulated Time-Dependent Climate Response to Solar Radiative Forcing Since 1600, *J. Geophys. Res.,* 104, 1973–1990, 1999.

Roeckner, E., K. Arpe, L. Bengtsson, M. Christoph, M. Claussen, L. Dumenil, M. Esch, M. Giorgetta, U. Schlese, and U. Schulzweida, The atmospheric gereneral circulation model ECHAM4: model description and simulation of present-day climate. Max-Planck-Institut fuer Meteorologie, Hamburg, Report No. 218, 1996.

Shindell, D. T., G. A. Schmidt, M. E. Mann, D. Rind, and A. Waple, Solar Forcing of Regional Climate Change During the Maunder Minimum, *Science,* 294, 2149–2152, 2001.

von Storch, H. and F. Zwiers, Statistical Analysis in Climate Research, *Cambridge Univ. Press*, UK, 1999.

Trenberth, K. E., and D. A. Paolino, Characteristic Patterns of Variability of Sea Level Pressure in the Northern Hemisphere, *Mon. Wea. Rev.*,109, 1169–1189, 1981.

Villalba, R., H. R. Grau, J. A. Boninsegna, G. C. Jacoby, and A. Ripalta, Tree-ring Evidence for Long-Term Precipitation Changes in Subtropical South America, *Int. J. Climatol., 18*, 1463–1478, 1998.

Widmann, M. and S. F.B. Tett, 2003, Simulating the climate of the Last Millennium. *PAGES Newsletter*, In press.

Wolff, J. O., Maier-Raimer, and S. Legutke, The Hamburg Ocean Primitive Equation Model, Technical Report, No 13, German Climate Computer Centre (DKRZ), Hamburg, 1997.

Zorita, E., and J. F. González-Rouco, Are Temperature-Sensitive Proxies Adequate for North Atlantic Oscillation Reconstructions? *Geophys. Res. Lett.*, 29, DOI 10.1029/2002GLO15404, 2002.

Zorita, E., J. F. González-Rouco, and S. Legutke, Testing the Mann et al. (1998) Approach to Paleoclimatic Reconstructions in the Context of a 1000-Yr Control Simulation with the ECHO-G Coupled Climate Model, *J. Climate*, 16, 1378–1390, 2003a.

Zorita, E., H. von Storch, J. F. González-Rouco, U. Cubasch, J. Luterbacher, S. Legutke, I. Fisher-Bruns, and U. Schlese, Simulation of the Climate of the Last Five Centuries. GKSS Report 2003/12, 2003b.